Chapter 22
Seismic Vulnerability Assessment of Slopes Along NH-1 Highway in Ladakh: A Comprehensive Study Using Rock Mass Classification and Seismic Slope Stability Analysis

Zaheer Abass, Vivek Padmanabha, Ashim Kanti Dey, and Gulzar Hussain

Abstract NH 1 has always been a national highway of high strategic importance, whether from a defense or civilian point of view. The highway connects Srinagar with Leh in Ladakh. Ladakh remains cut off for 5–6 months from the rest of the world from November to April due to heavy snowfall at Zojila Pass. The rock stability analysis along NH-1 is important for the smooth operation of traffic flow. The primary goal of this study is to carry out a geotechnical stability analysis along the NH-1D in Ladakh. The study was carried out with the help of a review of recent literature and relevant field tests. The methodology consists of calculating the rocks' Rock Mass Rating (RMS) values, followed by their kinematic analysis. The field studies consisted of the identification of instability-prone sites, the collection of discontinuity data, the assessment of groundwater conditions at 38 vulnerable locations from Kargil city 0 km to Leh town 211 km, and the carrying out of a point load test. A thorough geotechnical analysis improves our understanding of stability along the strategic highway. We had done rock slope stability analysis on 38 sites by using rock mass rating (RMR) followed by slope mass rating (SMR). Notably, 29% fall into the "fair" category, while 71% fall into the "good" category. However, there are a few sites like site 8 (19.3 km), site 13 (24.9 km), site 15 (27.5 km), site 18 (30.9 km), site 27 (115.2 km), and site 29 (117.2 km) that fall under the "marginally good" category. This classification indicates that many sites are prone to slope failure and require immediate measures against stability. We have selected site 9 (20.6 km), site 14 (25.6 km), site 16 (27.9 km), and site 28 (116.3 km), as these sites are very critical and prone to failure, to do numerical modeling under the static and dynamic load to

Z. Abass (✉) · V. Padmanabha
Civil Engineering Department, IIT Guwahati, Guwahati, India
e-mail: a.zaheer@iitg.ac.in

A. K. Dey
Civil Engineering Department, NIT Silchar, Silchar, India

G. Hussain
Geology Department Degree College Kargil, Kargil, India

R. Sarkar et al. (eds.), *Analyses for Retaining walls, Slope Stability and Landslides*,
Lecture Notes in Civil Engineering 568, https://doi.org/10.1007/978-981-96-1683-1_22

evaluate the seismic vulnerability of these slopes. To improve our knowledge, this study takes a novel approach involving seismic vulnerability assessment. Numerical modeling of selected sites uses historical earthquake data to simulate and analyze the slopes' response to earthquake loads. This comparative study aims to reveal the relationship between rock classification and seismic susceptibility, thereby providing valuable insights into slope behavior under earthquake loading conditions. The findings of this study not only contribute to the immediate need for stability measures along NH-1 and offer a novel perspective on how rock classification can be used as an early indicator of seismic susceptibility.

22.1 Introduction

Rock slope stability is a critical concern in the engineering world, particular in areas prone to earthquake. The stability in jointed, fractured rock does not depend only on the strength and orientation of slope, but the most influencing factors in rock mass are discontinuity, aperture, spacing, joint sets joint orientation, and ground water condition. For a complete understanding, it is imperative that we need to study deeper into the influence of additional properties of discontinuity, such as roughness, spacing, aperture, infill material, persistence, and groundwater conditions, on the slope stability in rock slope. The additional influencing parameters can be considered by stability of the slope from rock mass classification (RMR, GSI, etc.) perspectives. The study becomes further critical during dynamic and seismic conditions triggering devastating landslides, causing significant human and financial losses [1]. Therefore, it emphasizes the importance of assessing the seismic slope stability through rock mass classification.

Many researchers have done numerous studies on rock slope stability, yet accurately assessing its stability during earthquakes remains challenging. The failure of any slope during the earthquake depends on the material strength, slope orientation, and ground motion [2]. In practical engineering design, slope stability analysis is typically carried out using the limit equilibrium method (LEM), where the effect of earthquake loading is incorporated using an equivalent static inertia force [3]. Seismic slope stability analysis is more popularly initiated with the pseudo-static method [4], where the force experienced by the landslide during an earthquake predominantly depends on the seismic coefficient, represented by the intensity of the earthquake, weight of the soil/ rock mass that might fail. Hatzor et al. [5] have done the dynamic 2D stability analysis of upper terrace of King Herod's Palace in Masada, which is highly dominated by discontinuous fractured rock. Bhasin and Kaynia [6] have performed static and dynamic rock slope stability analysis for a 700 m high rock slope in western Norway using a numerical discontinuum modeling technique. Liu et al. [7] UDEC was used to study the dynamic response of Huangmail in the phosphorite rock slope in China under explosion.

In the present study, we propose a slope stability analysis based on a rigid plastic dynamic model and conduct finite element method (FEM) analysis incorporating

perspectives from rock mass classification and GSI. Our case study focuses on assessing rock slope stability at 4 sites. Site 9 (20.6 km), site 14 (25.6 km), site 16 (27.9 km), and site 28 (116.3 km) along NH1 in Ladakh.

22.2 Study Area and Geology

The study area, as depicted in Fig. 22.1a, is situated on the western periphery of the Tibetan Plateau and consists of an uphill cut slope along NH1 at various locations in Ladakh spanning from Kargil (34.570215, 76.125520) to Leh city (34.131015, 77.524403). The elevation in this area ranges from 3000 to 4000 m above mean sea level. The site location features incised valleys and mountain peaks are molded into narrow gorges without vegetation. The high altitude substantially affects the region's geotechnical properties, such as soil, rock characteristics, and slope stability. Ladakh has an arid and frigid climate, with temperatures between −30 degrees Celsius in December and January to + 30 degrees Celsius in June–August. The region consists primarily of sedimentary and metamorphic rocks, with some volcanic formations present on the eastern side.

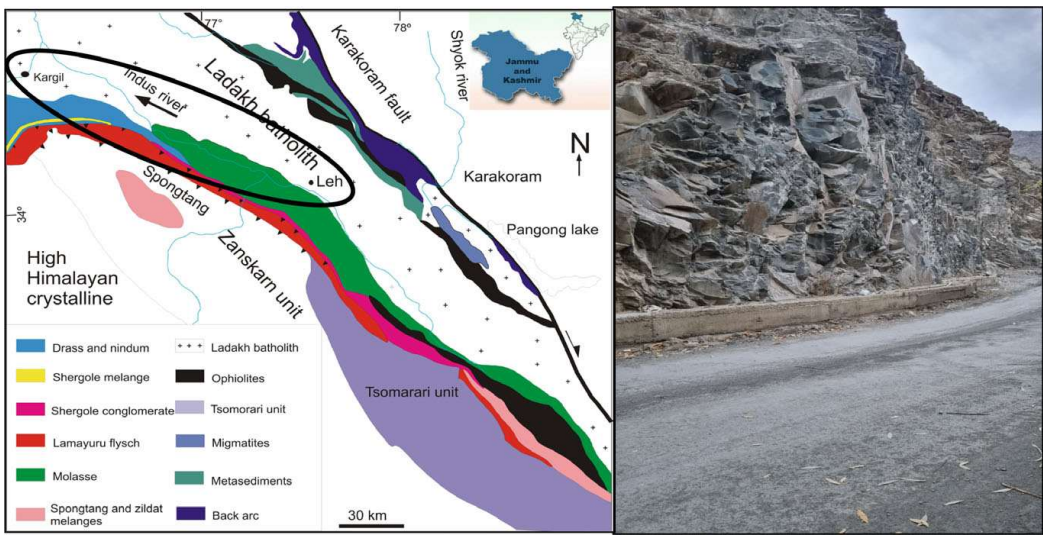

Fig. 22.1 **a** Geological map of Ladakh-Zanskar (modified after [8]), **b** highly fractured facets prone to failure

22.2.1 Rock Mass Rating (RMR)

A geomechanical classification system, rock mass Rating (RMR), developed by Bieniawski [9], considers several geological factors that influence slope stability. These factors are assigned ratings, and the sum of these ratings is known as the RMR basic value, which reflects the overall stability of the rock mass.

- Uniaxial compressive strength (UCS) of rock/point load index.
- Rock quality designation (RQD).
- Spacing of discontinuity.
- Condition of discontinuity.
- Ground water condition.

Point load strength was calculated from the laboratory by using Eq. (22.1) of all the lump samples collected from the site according to the guidelines provided (BIS 8764: 1998),

$$I_1(50) = \frac{P}{(\mathrm{DW})^{0.75}\sqrt{D^*}}, \tag{22.1}$$

where I_1 (50) = Point load strength of lump (Mpa)
P= Peak load at failure in kN/mm^2
D= Mean cross-sectional of lump (mm)
W= Mean width of lump (mm)
D^* = Standard size of lump (50 mm).

Rock quality designation (RQD) was estimated by using Eq. (22.2) [10].

$$\mathrm{RQD} = 110 - 2.5(\mathrm{Jv}), \tag{22.2}$$

where Jv is the volumetric joint count, measures joints per meter cube of rock mass, and can be estimated using Eq. (22.3).

$$\mathrm{Jv} = \sum_{i=1}^{j} \frac{1}{s_i}, \tag{22.3}$$

where s_i (m) is the average joint set spacing for the ith joint set, and j is the total number of the joint sets except random joint sets (Table 22.1).

22.2.2 Geological Strength Index (GSI)

This classification system was first introduced by [11] for all types of rock masses. GSI was estimated by using the correlation Eq. (22.4) (IS: 13365).

Table 22.1 Rock mass ratings at several study sites

Site no.	Point load strength	RQD	Joint spacing ratting	Joint condition rating	Ground water condition	RMR basic	Rock mass description
–	Rating values					–	–
9	7	8	8	17	7	47	Fair rock
14	12	13	8	17	10	60	Fair rock
16	12	8	8	13	15	56	Fair rock
28	12	17	8	14	15	66	Good rock

$$\text{GSI} = \text{RMR} - 5, \text{GSI} \geq 18 \text{or} \text{RMR} \geq 23 \tag{22.4}$$

We used GSI to determine the generalized Hoek–Brown criterion. We did the numerical modeling on RS2 software (Rocscience, Toronto, Canada version 11.021 September 13 2023). To calculate the Hoek–Brown criterion for estimating the rock mass strength properties, we used Eq. (22.5).

$$\sigma_1 = \sigma_3 + \sigma_{ci}\left(\text{mb}\frac{\sigma_3}{\sigma_{ci}} + s\right)^a, \tag{22.5}$$

where σ_1 and σ_3 are the principal stresses at the point of failure, σ_{ci} is the UCS of intact rock, mb is the reduced value of m_i material constant, and s, a are the material constants for the rock mass.

22.3 Kinematic Analysis and Numerical Modeling

Kinematic analysis is based on the orientation of the discontinuity of the slope. It is based on Markland's test, introduced by Markland in 1972, and is most commonly used to assess rock slope stability. It involves identifying the potential mode of failure by analyzing the geometry and orientation of discontinuity. We used Dip's software (Rocsicence) to perform a kinematic analysis on the selected sites. Three different modes of failure could slope fail under different condition, planar, wedge, and toppling modes of failure. The slope fails in planar mode when the slope's direction matches the failure plane direction in between ±20°, and the slope angle is steeper than the failure plane dip but less than the angle of internal friction. For the wedge mode of failure, the angle difference between the direction where two discontinuity planes intersect, and the slope face tilt must be less than 20°. The plunge of the intersecting line should be less than the slope's inclination but more significant than the friction angle. In the case of toppling failure mode, the strike of the discontinuity, then basal plane separation, and the slope's face separation plane need to be parallel or tilted by not more than 10°.

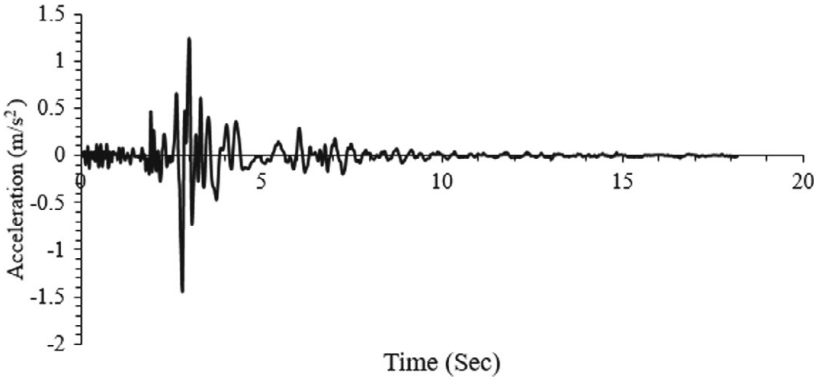

Fig. 22.2 Acceleration time history for Chamba earthquake (March 24, 1995, Mb = 4.9) after [13]

Whereas RS2 software was used for numerical analysis (FEM). We have adopted 6 noded triangular plain strain elements used for discretization. For analysis under the static load condition, the boundary condition was fixed to support the base and sides of the model (restrained against horizontal and vertical directions), and the slope face was kept free. The shear reduction approach has been adopted, where the material's shear strength reduces until the slope's shear strength fails to converge [12]. Dynamic boundary conditions were adopted for analysis under the earthquake load (Chamba earthquake March 24, 1995, Mb = 4.9). Figure 22.2 shows the acceleration versus time graph, and time history data was used to assess the seismic vulnerability of the slopes in these models as a load. A Hoek–Brown failure criterion was used to perform the numerical analysis.

22.4 Results and Discussion

22.4.1 Results of Kinematic Analysis

See (Fig. 22.3)

Site 9. This site is mainly exposed to basaltic rock and is 19.3 km from Kargil town. Joint orientation is given in Table 22.2. The kinematic analysis of the joint and slope data at this revealed that potentially two types of failure could occur. The toppling failure will occur along (J4) because J4 is dipping into the slope face, and wedge failure is likely to occur along joint set (J1 and J3) because the dip angle of J1 and J3 is greater than the angle of internal friction and less than the slope angle. The trend and plunge of the wedge are $N263°$ AND 58°.

Site 14. This site is located at 25.6 km from Kargil town. This site is exposed to basaltic rock type; three primary joint sets plus random joints are there. The kinematic analysis inferred that there could be a toppling mode of failure and will be along J3 because J3 is sub-parallel and dipping into the slope face.

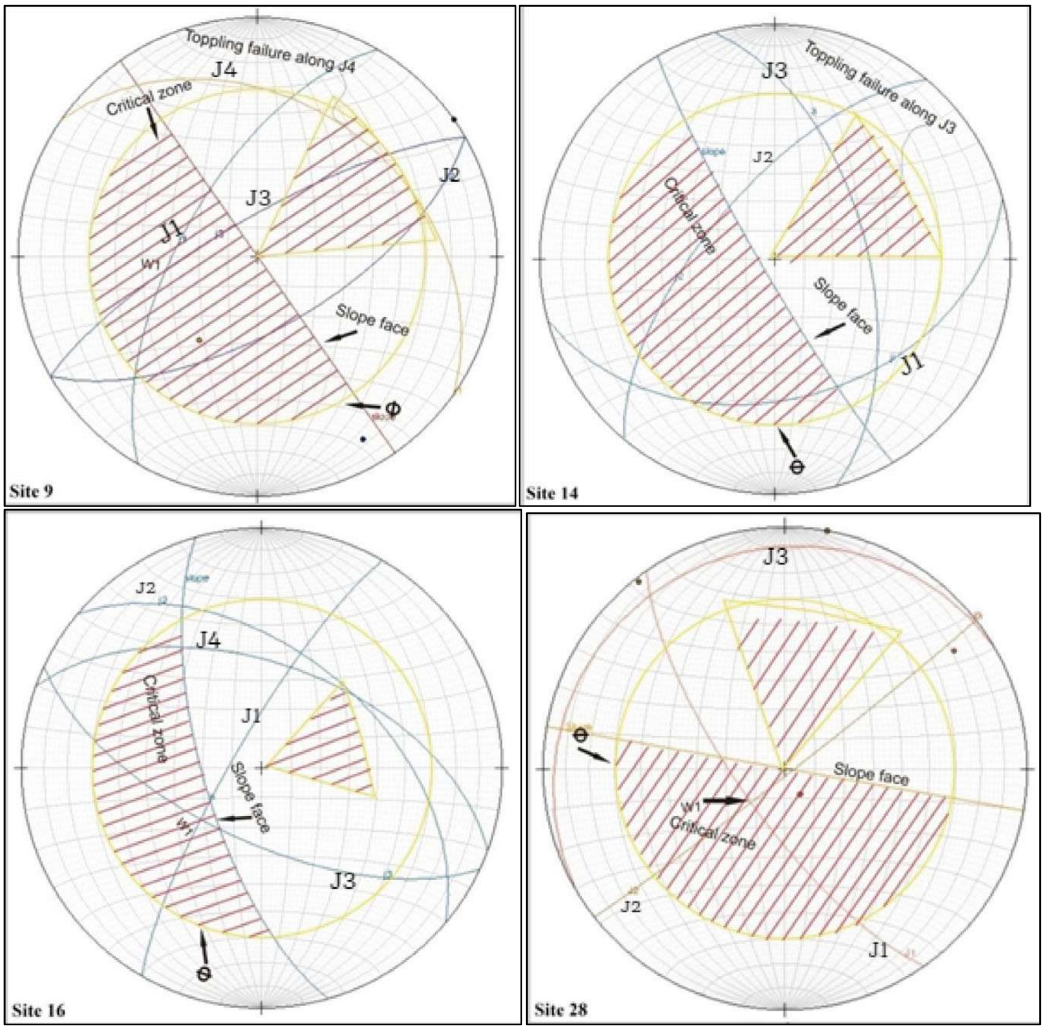

Fig. 22.3 Stereographic plots of discontinuities and slopes for sites 9, 14, 16, and 28

Table 22.2 Data on various joint parameters

Site	Location milestone km	Orientation of discontinuities (Dip direction/amount)				Orientation of slope (Dip direction/amount)
–	–	J1	J2	J3	J4	–
Site 9	20.6 km	N300°/64°	N150°/65°	N330°/77°	N33°/35°	N235°/90°
Site 14	25.6 km	N165°/40°	N310°/66°	N75°/58°	–	N240°/85°
Site 16	27.9 km	N300°/80°	N40°/50°	N205°/65°	N20°/54°	N254°/70°
Site 28	116.3 km	N235°/74°	N142°/88°	N330°/10°	–	N190°/90°

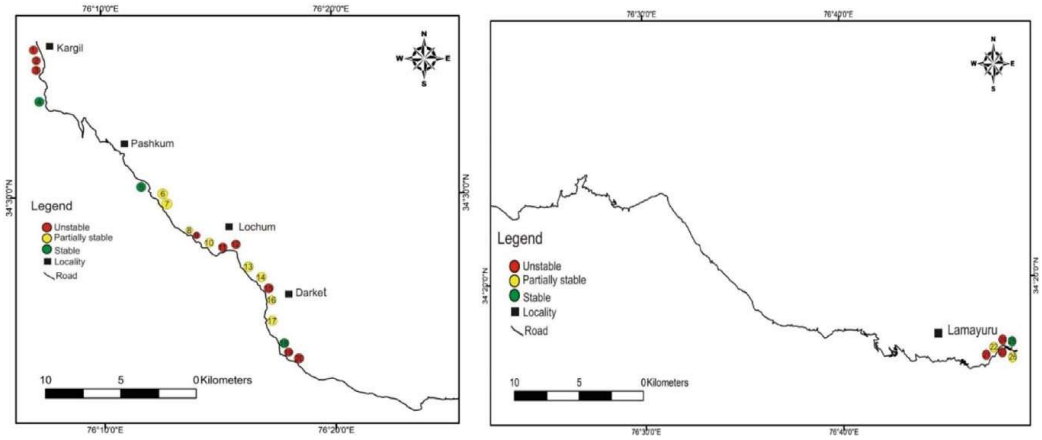

Fig. 22.4 Location and stability condition of the study area

Site 16. This site is located at 27.9 km and comprises of basaltic rock. Moreover, it estimated from the kinematic analysis that there could be wedge mode of failure that could occur at this site as the intersection of J1 and J3 because the plunge of the line of intersection is less than the dip angle of slope. The trend and plunge of the wedge failure are $N229°$ and 62°.

Site 28. This site is located 113.4 km from Kargil and is exposed to moderately weathered volcanic rock. The kinematic analysis revealed there could be wedge failure due to the intersection of J1 and J2, and the trend and plunge for the wedge is $N223°$ and 73° (Fig. 22.4).

22.4.2 Numerical Modeling

The RS2 software is used for numerical analysis. The geometry considered for the numerical analysis is shown in Fig. 22.5. Strength reduction factor (SRF) represents the actual strength of the slope to the model strength at the point of failure corresponds to the factor of safety when the slope fail. According to [4], we should attain a minimum safety factor of 1.50 for a cut slope. If the factor of safety lies between 1 and 1.50, then it is partially stable; more than 1.50 is stable, and the higher the SRF will indicate a higher factor of safety. In our model, the geotechnical parameter was established from the site-specific RMR sheet; in the absence of data, the value of parameters was estimated from the rock data library RS Data software (Rocscince, Toronto, Canada) with the help of RMR data. The input parameter used for analysis is given in Table 22.3.

Finite element analysis (FEA) was done under two different conditions on RS2 software; first, strength reduction analysis was done under the gravity load results given in Table 22.4, and then we did the nonlinear dynamic analysis.

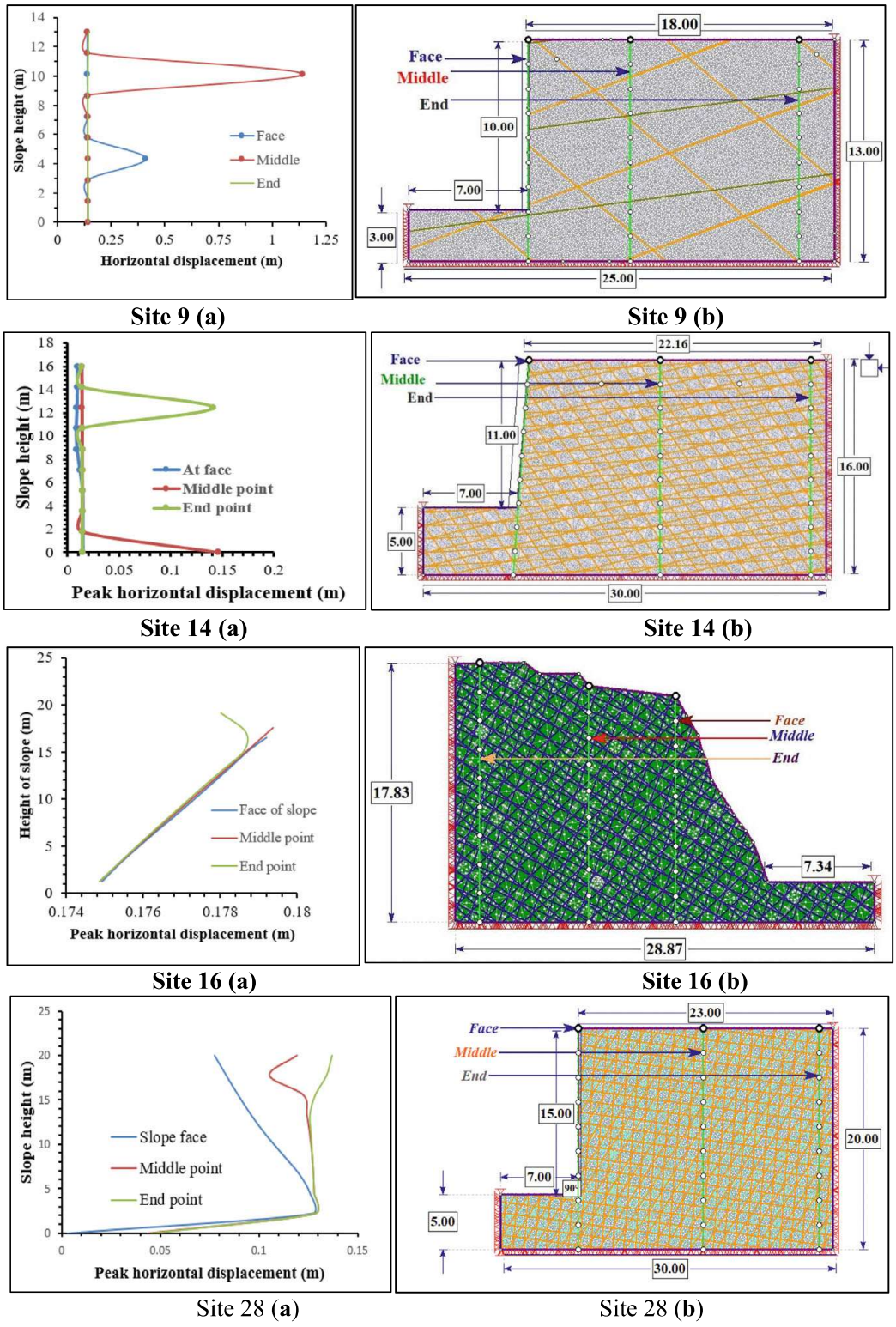

Fig. 22.5 Peak horizontal displacement at critical point, face, middle, and end (left) and slope geometry joint orientation (right)

Table 22.3 Input parameter for analysis

Properties	Site 9	Site 16	Site 14	Site 28
Uniaxial compressive strength (Mpa)	78	175	152	168
GSI	42	51	55	61
m_i	28	28	25	25
s	0.15	0.82	0.14	0.35
cohesion c(Mpa)	2.12	3.51	3.82	4.35
angle of internal friction$\emptyset$(°)	29.3	41.7	43.5	40.3

Table 22.4 Result of FEA under static and dynamic load condition

Site. No.	Achieved FOS in static case	Achieved FOS in the dynamic case
Site 9	1.35	0.86
Site 14	0.88	0.66
Site 16	9.25	5.25
Site 28	0.96	0.58

Among all the sites, site 9 is partially stable under the gravity load, and other slopes need to be stabilized as the strength reduction factor is less than one; different types of remedial measures can be used to stabilize the slope.

Further, we estimated the slope displacement under the dynamic loading condition using the time history data of (the Chamba earthquake on March 24, 1995, Mb = 4.9). We estimated the displacement by using nonlinear dynamic analysis; a time query line of 10 points was created at three places of the model, firstly on the face, second on the middle, and third on the back end of the slope, and estimated the peak displacement and acceleration amplification on each point.

In Fig. 22.5, site 9(a) shows the peak horizontal displacement of 1.13 m at the height of 10.11 from the bottom of the model, and this is the point of intersection of joints where high displacement is shown. Figure 22.5, site 9(b) shows the slope geometry and joint orientation. Figure 22.5 site 14(a) shows the peak displacement of 0.140 m at a height of 12.44 m from the bottom of the model. Similarly, Fig. 22.5 site 16(a) shows a peak displacement of 0.179 m at the height of 17.55 m from the bottom of the model, and similarly, Fig. 22.5 site 28(a) shows a maximum displacement of 0.137 m at the height of 20 m from the bottom of the model. Among all the studied slopes, all the models show higher displacement at the upper height of the model and at the second-time query line, which lies approximately at the middle of the slope; this infers that there could probably be a wedge mode of failure.

22.5 Conclusion

This study investigated the static and seismic vulnerability of four critical rock slopes along NH1 in Ladakh from Kargil to Leh using kinematic analysis and finite element analysis based on the plastic rigid dynamic model using the Hoek–Brown failure criterion. Rock mass classification was performed using rock mass rating (RMR) and geological strength index (GSI) for these sites.

The key findings are:

- This study provides a comprehensive seismic vulnerability assessment of various sites along NH1 in Ladakh, integrating rock mass classification and geological strength index (GSI) with seismic slope stability.
- Site **28**, with the second highest compressive strength of **168** Mpa among the four studied sites, shows the lowest SRF of **0.58**. This proves that the role of stability in the research area is primarily controlled by the slope angle and the orientation of discontinuity rather than the condition of the rock.
- Kinematic analysis revealed potential failure modes for each site.
- Nonlinear dynamic analysis using the time acceleration history data of the Chamba earthquake (1995) showed the peak horizontal displacement occurring at various points. This suggests a potential for wedge, toe, and toppling-type failure mode under the seismic event.

This study shows that the slopes along NH1 at many places are steep and composed of loose or fractured with different discontinuity orientations. This problem can lead to hazards that can endanger human life and property. Therefore, mitigation measures must be implemented to reduce the risk of rock slope failure.

References

1. Ansarin MK, Ahmad M, Singh R, Singh TN (2012) Rockfall assessment near Saptashrungi Gad Temple, Nashik, Maharashtra, India. Int J Disaster Risk Reduct 2(1):77–83
2. Hack R et al (2007) Influence of earthquakes on the stability of slopes. Eng Geol 91(1):4–15
3. Kawajiri S et al (2023) Geotechnical characteristics and seismic stability evaluation of pumice-fall deposits soil on collapse slope by the 2018 Hokkaido eastern Iburi earthquake
4. Hoek E, Bray J (1981) Rock slope engineering 358
5. Hatzor YH, Arzi AA, Zaslavsky Y, Shapira A (2004) Dynamic stability analysis of jointed rock slopes using the DDA method: king Herod's Palace, Masada, Israel. Int J Rock Mech Min Sci 41(5):32–813
6. Bhasin R, Kaynia AM (2004) Static and dynamic simulation of a 700-m high rock slope in Western Norway. Eng Geol 71(3-4):26–213
7. Liu YQ, Zhao J, Li JR, Zhou QC (2004) UDEC simulation for dynamic response of a rock slope subject to explosions. Int J Rock Mech Min Sci 41(3):3–8
8. Mahéo G, Bertrand H, Guillot S, Mascle G, Pêcher A., Picard C, De Sigoyer J (2000) Témoins d'un arc immature téthysien dans les ophiolites du Sud Ladakh (NW Himalaya, Inde). Comptes Rendus de l'Académie des Sciences-Series IIA-Earth and Planetary Science 330(4):289–295
9. Bieniawski ZT (1973) Engineering classification of jointed rock masses. Trans S Afr Inst Civ Eng, 15:355–344